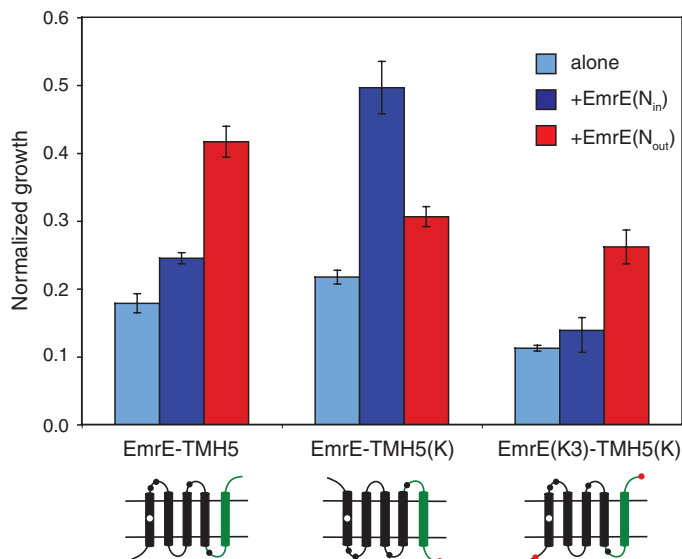


**Fig. 3.** Topological effects of adding Lys residues to the N- and C-termini of the EmrE-TMH5 construct (Glu<sup>14</sup> is retained in these constructs). TMH5 (green in the miniature cartoons) is a GGPG...GPGG-flanked 19-residue-long segment composed of four Leu and 15 Ala. Normalized growth values during coexpression with EmrE(N<sub>in</sub>) (blue bars) and EmrE(N<sub>out</sub>) (red bars) are shown. Error bars indicate  $\pm 1$  SEM.



protein when coexpressed with EmrE(N<sub>out</sub>) (Fig. 2B). This appeared to be a result of the charge and not the length of the C-terminal tail, because the addition of up to six Gly had little effect on the dual topology of EmrE (fig. S2).

Finally, to examine whether a C-terminal positively charged residue could influence the global topology when moved even farther from the N terminus, we extended EmrE by adding a fifth TMH, composed only of alanines and leucines, to the C terminus. Given its composition, this TMH was not expected to interact in any specific way with TMHs 1 to 4. EmrE-TMH5 had an N<sub>in</sub> topology, as it was inactive when expressed alone but imparted EtBr resistance—albeit at a lower level than wild-type EmrE—when coexpressed with EmrE(N<sub>out</sub>) (Fig. 3). However, adding a C-terminal Lys to EmrE-TMH5 resulted in a protein [EmrE-TMH5(K)] that imparted EtBr resistance only when coexpressed with EmrE(N<sub>in</sub>). Thus, the C-terminal Lys can reverse the orientation of as many as five upstream TMHs. Finally, the N<sub>in</sub> topology was regained when the C-terminal Lys was complemented with an N-terminal Lys [EmrE(K3)-TMH5(K)].

In summary, the membrane orientation of the 4-TMH, dual-topology protein EmrE and a 5-TMH version of the same protein could be shifted both to N<sub>in</sub> and to N<sub>out</sub> by adding a single positively charged residue in various locations throughout the protein. In all cases, the shift in orientation was as predicted by the positive-inside rule. A C-terminal Arg or Lys was as effective in this regard as were positively charged residues placed in other locations closer to the N terminus. Apparently, the protein remains “topologically uncommitted” until the last residue has been synthesized. These and other observations of a related kind (17) raise important questions regarding the mechanism of membrane protein insertion and assembly. Specifically, how much protein can the translocon pore accommodate? Are translocon-associated proteins, such as YidC (18), involved

in chaperoning membrane proteins to their final topology? Is postinsertion conversion between different topologies, so far seen only under conditions of extreme alterations in membrane lipid composition (17), possible also in wild-type cells?

#### References and Notes

1. G. von Heijne, *EMBO J.* **5**, 3021 (1986).
2. G. von Heijne, *Nature* **341**, 456 (1989).
3. G. Gafvelin, G. von Heijne, *Cell* **77**, 401 (1994).
4. M. Monné, G. Gafvelin, R. Nilsson, G. von Heijne, *Eur. J. Biochem.* **263**, 264 (1999).
5. G. von Heijne, *Nat. Rev. Mol. Cell Biol.* **7**, 909 (2006).
6. W. R. Skach, *Nat. Struct. Mol. Biol.* **16**, 606 (2009).

7. M. Bogdanov, J. Xie, P. Heacock, W. Dowhan, *J. Cell Biol.* **182**, 925 (2008).
8. S. Schuldiner, *Biochim. Biophys. Acta* **1794**, 748 (2009).
9. I. Ubarretxena-Belandia, J. M. Baldwin, S. Schuldiner, C. G. Tate, *EMBO J.* **22**, 6175 (2003).
10. Y. J. Chen *et al.*, *Proc. Natl. Acad. Sci. U.S.A.* **104**, 18999 (2007).
11. M. Rapp, S. Seppälä, E. Granseth, G. von Heijne, *Science* **315**, 1282 (2007).
12. T. Nara *et al.*, *J. Biochem.* **142**, 621 (2007).
13. I. Nasie, S. Steiner-Mordoch, A. Gold, S. Schuldiner, *J. Biol. Chem.* **285**, 15234 (2010).
14. M. Rapp, E. Granseth, S. Seppälä, G. von Heijne, *Nat. Struct. Mol. Biol.* **13**, 112 (2006).
15. Materials and methods are available as supporting material on Science Online.
16. E. Padan, D. Zilberstein, S. Schuldiner, *Biochim. Biophys. Acta* **650**, 151 (1981).
17. W. Dowhan, M. Bogdanov, *Annu. Rev. Biochem.* **78**, 515 (2009).
18. K. Xie, R. E. Dalbey, *Nat. Rev. Microbiol.* **6**, 234 (2008).
19. H. Yerushalmi, S. S. Mordoch, S. Schuldiner, *J. Biol. Chem.* **276**, 12744 (2001).
20. We thank Ann-Louise Johansson for technical assistance. This work was supported by grants to G.v.H. from the European Research Council (ERC-2008-AdG 232648), the Swedish Cancer Foundation, the Swedish Research Council, and the Swedish Foundation for Strategic Research, to J.S.S. from the International Human Frontier Science Program Organization, and to P.L.G. from the European Communities (TransSys PITN-2008-215524).

#### Supporting Online Material

www.sciencemag.org/cgi/content/full/science.1188950/DC1  
Materials and Methods  
Figs. S1 and S2  
References

1 March 2010; accepted 4 May 2010  
Published online 27 May 2010;  
10.1126/science.1188950  
Include this information when citing this paper.

## A Generalization of Hamilton's Rule for the Evolution of Microbial Cooperation

jeff smith,\*† J. David Van Dyken, Peter C. Zee

Hamilton's rule states that cooperation will evolve if the fitness cost to actors is less than the benefit to recipients multiplied by their genetic relatedness. This rule makes many simplifying assumptions, however, and does not accurately describe social evolution in organisms such as microbes where selection is both strong and nonadditive. We derived a generalization of Hamilton's rule and measured its parameters in *Myxococcus xanthus* bacteria. Nonadditivity made cooperative sporulation remarkably resistant to exploitation by cheater strains. Selection was driven by higher-order moments of population structure, not relatedness. These results provide an empirically testable cooperation principle applicable to both microbes and multicellular organisms and show how nonlinear interactions among cells insulate bacteria against cheaters.

Social evolution has illuminated many different areas of biology, from altruistic behavior in insects to sex ratios, selfish genetic elements, and multicellularity (1, 2). The central puzzle in this field is how cooperation—

increasing the fitness of other individuals—persists when cheaters can benefit without paying the cost of cooperating. The most prominent explanation for the evolution of cooperation is kin selection, in which benefits preferentially

go to individuals who share cooperation alleles (3, 4). The centerpiece of kin selection theory is Hamilton's rule (3, 5, 6). It states that cooperation will evolve if  $rb - c > 0$ , where  $b$  is the benefit of cooperation;  $c$  is the cost of cooperation; and  $r$  is the genetic relatedness of actors to recipients (Fig. 1A). Kin selection relatedness is a statistical regression coefficient describing the similarity of actors and recipients at relevant cooperation loci and is not necessarily equal to whole-genome similarity (5–7).

Hamilton's rule is an elegant evolutionary principle, but it encounters problems when selection is strong and fitness effects are nonadditive (5, 8). Nonadditivity occurs whenever fitness is a nonlinear function of social environment (Fig. 1B) or when different genotypes have different slopes (Fig. 1C). Under these circumstances,  $b$  and  $c$  are functions of  $r$  (9). This confounds fitness effects with population structure, obscures the biological causes of selection, and limits the usefulness of Hamilton's rule as an interpretive tool (fig. S1). It also makes it difficult to test kin selection with Hamilton's rule, because costs and benefits cannot be extrapolated to other population structures. Social evolution needs theory that makes testable predictions for specific systems (10, 11).

These problems are especially pronounced for cooperation among microbes. Microbial traits as diverse as quorum sensing, biofilms, development, metabolism, mutualism, and virulence are social and vulnerable to cheating (11–18). Many

Department of Biology, Indiana University, Bloomington, IN 47405, USA.

\*Present address: Department of Ecology and Evolutionary Biology, Rice University, Houston, TX 77005, USA.

†To whom correspondence should be addressed. E-mail: smith74@indiana.edu

systems show strong frequency-dependent selection, one form of nonadditivity (12, 14, 16–18). So far, social evolution theory has mostly been a qualitative, heuristic guide to interpretation. Models are seldom compared with data, and attempts to measure Hamilton's rule are rare [but see (19, 20)]. Even though microbes have been singled out as important tests of social evolution theory (11), it is still unclear how much relatedness is required to prevent cheaters from spreading, whether relatedness in natural populations is sufficient, and whether kin selection acts differently in microbes and in animals.

To bridge the gap between theory and data, we derived a generalization of Hamilton's rule that does not assume additivity or weak selection and whose parameters are empirically measurable (21). We found that cooperators increase in frequency if

$$\mathbf{r} \cdot \mathbf{b} - c + \mathbf{m} \cdot \mathbf{d} > 0 \quad (1)$$

Distributions can be described by their moments: parameters that measure their shape and

location. The relatedness vector  $\mathbf{r} = \{r_1, r_2, \dots\}$  measures how the distributions of social environments encountered by cooperators and noncooperators differ in each of these moments (fig. S2).  $r_1$  is equivalent to  $r$  in Hamilton's rule (5). The other terms are higher-order relatedness coefficients (22, 23). Any smooth function can be expanded into a Taylor polynomial series whose coefficients measure its linear, quadratic, and higher-order components. The benefit vector  $\mathbf{b}$  describes noncooperator fitness as a function of social environment (red lines in Fig. 1) in terms of its Taylor coefficients.  $c$  is the cost of cooperation when all neighbors are noncooperators.  $\mathbf{m} \cdot \mathbf{d}$  is nonzero when benefits depend on recipient genotype (Fig. 1C).  $\mathbf{m}$  is the moments vector for cooperators.  $\mathbf{d}$  is the difference between the Taylor series of cooperators and noncooperators. Unlike Hamilton's rule, Eq. (1) disentangles fitness effects from population structure and is valid for arbitrarily complex forms of social selection. When fitness effects are additive, Eq. (1) reduces to  $rb - c > 0$ .

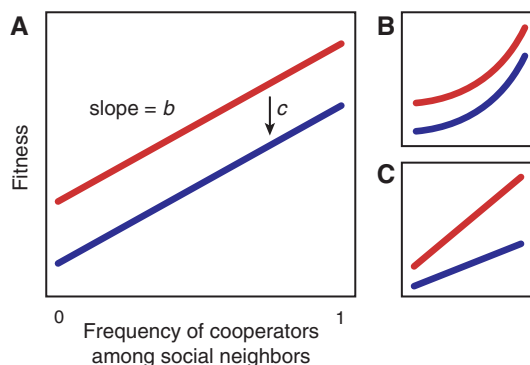
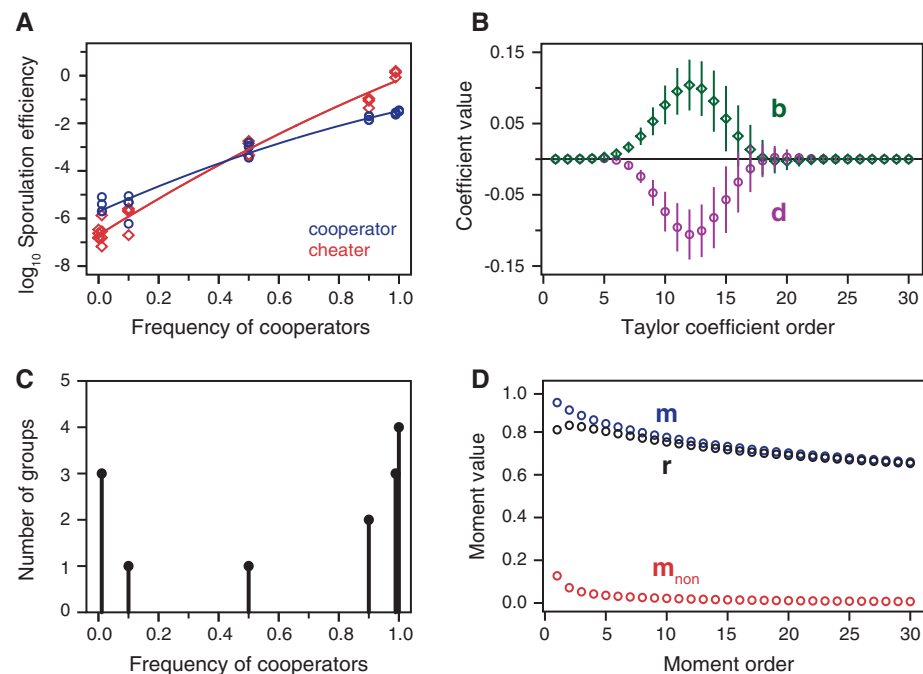


**Fig. 1.** Measuring the costs and benefits of cooperation in microbes. Blue, cooperator fitness; red, noncooperator fitness. (A) In Hamilton's rule,  $b$  is the slope of fitness against the frequency of cooperators among social neighbors;  $c$  is the fitness difference between cooperators and noncooperators for a given social environment. Fitness effects are non-additive when benefits are (B) nonlinear or (C) depend on recipient genotype.

**Fig. 2.** Parameters of the generalized Hamilton's rule measured in an experimental population of sporulating *Mycobacterium* bacteria. (A) Absolute fitness of a cooperator strain (blue circles) and a cheater strain (red diamonds) as a function of their frequency within groups. Data points are independent experimental replicates; lines, regression model fit to data. (B) Fitness terms in Eq. (1), calculated from the data shown in (A). Green diamonds, benefit vector  $\mathbf{b}$ ; purple circles, genotype-dependence vector  $\mathbf{d}$ . Points show best-fit model ( $\pm$ SD from bootstrapped data). (C) Initial distribution of cooperators among groups for a specific experimental population. (D) Social structure terms in Eq. (1) were calculated for the population shown in (C). Blue, cooperator moments  $\mathbf{m}$ ; red, noncooperator moments  $\mathbf{m}_{\text{non}}$ ; black, relatedness vector  $\mathbf{r}$ .



We applied our generalized rule to data from experimental populations of *Myxococcus xanthus* bacteria. When starved of amino acids, *M. xanthus* cells aggregate and form fruiting bodies in which a small fraction of cells become stress-resistant spores; the rest die (24). Some cheater strains sporulate superefficiently among cooperators but do poorly on their own (14). We mixed a cooperator strain and a cheater strain at different frequencies, let them develop, and measured their abundance among surviving spores. Fitness effects were strongly nonadditive (Fig. 2A). Cooperators increased the fitness of both genotypes [ $F_{(1,43)} = 1872.92$ ,  $P < 0.0001$ ;  $n = 48$ ], but the effect was strongly nonlinear [slightly less than exponential;  $F_{(1,43)} = 15.69$ ,  $P < 0.001$ ]. Cheaters benefited more than cooperators [ $F_{(1,43)} = 81.87$ ,  $P < 0.0001$ ]. Cooperators were more fit than cheaters at low frequencies [ $F_{(1,43)} = 51.54$ ,  $P < 0.0001$ ] but less fit at high frequencies. Cooperating was therefore altruistic when locally common but mutually beneficial when rare (25).

We calculated **b** and **d** in Eq. (1) from the Taylor series of the fitted statistical model and found that their linear, additive components were very small (Fig. 2B). The largest terms were order 10 to 15. This is caused by the steepness of the curves in Fig. 2A and means that fitness was disproportionately determined by groups with high frequencies of cooperators. The genotype of individual neighbors mattered less than the genotype of several neighbors collectively. Under such circumstances, the most important components of population structure are the corresponding higher-order moments—not first-order relatedness.  $c$  was  $-1.73 \pm 0.02$  (SEM)  $\times 10^{-6}$ . A negative cost indicated that cooperation provided a direct fitness benefit when most neigh-

bors were noncooperators. This was a minor component of fitness, however. Large negative values of **d** indicated that cheaters mainly gain advantage by benefiting from cooperative groups more than cooperators do.

We calculated **r** and **m** for an experimental population where most groups contained both genotypes, but with a strong skew toward one or the other (Fig. 2C). The components of these vectors varied less than those of **b** and **d** (Fig. 2D). Kin selection relatedness was  $r_1 \approx 0.8$ . Putting it all together, the predicted inclusive fitness effect of cooperation was  $\mathbf{r} \cdot \mathbf{b} - c + \mathbf{m} \cdot \mathbf{d} = 0.014$  spores per cell [95% confidence interval (CI) 0.004 to 0.021], which did not significantly differ from the observed value of 0.0135. A positive inclusive fitness effect indicated that, in this population, kin selection favored cooperation.

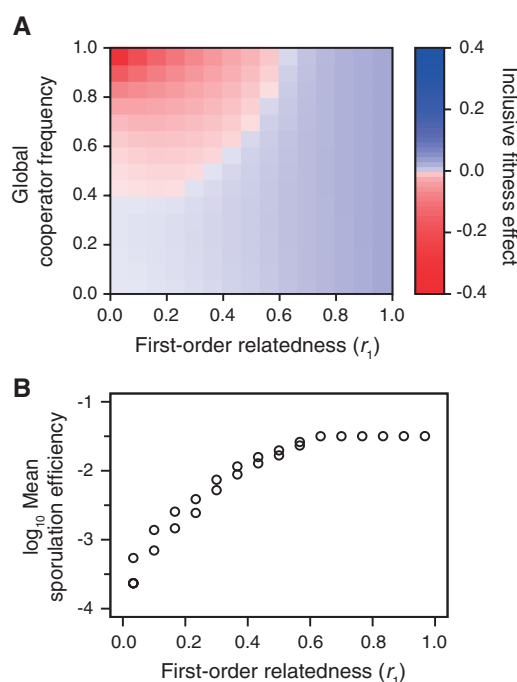
To better understand kin selection in this system, we calculated the inclusive fitness effect for populations with different global cooperator frequencies and rates of migration between groups. We found that cooperative development in *M. xanthus* is markedly resilient to cheating. In the conventional island model of population structure (26), cheaters could invade populations of cooperators only if migration was high enough that  $r_1 < 0.6$  (Fig. 3A). Considering the large fitness advantage cheaters often had within groups, this is a remarkably low relatedness threshold. Reexamining Fig. 3A gives an intuitive explanation for this result. Compared with cooperators in all-cooperator groups, cheaters had a net advantage only in groups with >70% cooperators. Population structure limits the abundance of groups in this narrow range of frequencies (fig. S2). The specific form nonadditivity takes is crucial. Increasing returns from cooper-

ation limit the ability of cheaters to invade, whereas decreasing returns make it easier (fig. S3). When population structure was very low, direct fitness benefits allowed cooperators to escape being displaced by cheaters. Instead, both genotypes coexisted in a balanced polymorphism (Fig. 3A). Population structure reduced the equilibrium frequency of cheaters and their effect on population mean fitness (“cheater load”) (Fig. 3B). Selection was frequency dependent because the higher-order components of population structure that dominate selection were also frequency dependent (fig. S4). Hamilton’s rule, however, misleadingly placed the cause of frequency dependence in its fitness terms  $b$  and  $c$  instead of its population structure term  $r$  (fig. S4).

Our generalization of Hamilton’s rule provides a kin selection principle that is valid for systems with strong nonadditive fitness effects. It shows why higher-order moments of population structure appear in models of social evolution (23, 27), shows when they are important, and provides a general method for handling them. Because Eq. (1) refers only to fitness and genotype frequencies, it is independent of many system-specific details and can be applied to cooperation at all levels of biological organization—not just microbes. It also lets social evolution theory be more than a heuristic guide to interpretation. Because all the terms in Eq. (1) are empirically measurable, it is both a quantitative analytical tool and a testable hypothesis. The inclusive fitness effect ( $\mathbf{r} \cdot \mathbf{b} - c + \mathbf{m} \cdot \mathbf{d}$ ) is a quantitative measure of selection that one can use to compare different hypothetical mechanisms for the evolution of cooperation. One could, for example, evaluate the relative importance of population structure and infectious transfer of cooperation genes (28) by comparing the amount of allele frequency change due to kin selection or gene transfer. The inclusive fitness effect also shows when “Trojan horse” strategies for controlling microbial infections with human-introduced cheaters (29) are likely to be successful.

Strong nonadditivity plays an important role in microbial cooperation. It causes these systems to deviate from the traditional scheme where social interactions are classified as altruistic, mutually beneficial, selfish, or spiteful (24, 25). Frequency-dependent selection within groups can create situations where cooperation is altruistic at some frequencies but mutually beneficial at others (Fig. 2A). With nonadditivity, the  $r$  in Hamilton’s rule can also be a relatively unimportant component of population structure. In our *M. xanthus* system, selection is primarily determined by higher-order terms that measure the abundance of groups with high frequencies of cooperators. Finally, strong population structure is not always needed to prevent the spread of strong cheaters. The cheater strain we examined has a hundred-fold fitness advantage within groups when it is rare, and it massively reduces

**Fig. 3.** *M. xanthus* development is resilient to cheating. **(A)** Conditions under which kin selection favors cooperation. Blue signifies conditions in which cooperators have higher mean fitness than cheaters; red, cheaters have higher mean fitness. In an island model of population structure, cheaters invade only when migration between groups is large enough that first-order relatedness is  $< 0.6$ . When cheaters can invade, they reach an equilibrium frequency where cooperators remain at least 40% of the population. We report population structure in terms of first-order relatedness instead of migration rate to aid comparison with other systems. **(B)** Cheater load. Points show population mean fitness near the selective equilibrium for a given level of population structure.



group fitness when it is common. Nevertheless, increasing-returns nonadditivity allows cooperation to evolve at levels of population structure comparable to that seen among social insect colonies (30). Cheaters have a rare advantage in several systems (12, 16–18) and may be a common property of microbial cooperation.

#### References and Notes

- J. Maynard Smith, E. Szathmari, *The Major Transitions in Evolution* (Oxford Univ. Press, New York, 1995).
- L. Keller, Ed., *Levels of Selection in Evolution* (Princeton Univ. Press, Princeton, NJ, 1999).
- W. D. Hamilton, *J. Theor. Biol.* **7**, 1 (1964).
- A. S. Griffin, S. A. West, *Trends Ecol. Evol.* **17**, 15 (2002).
- D. C. Queller, *Evolution* **46**, 376 (1992).
- P. D. Taylor, S. A. Frank, *J. Theor. Biol.* **180**, 27 (1996).
- A. Grafen, *Oxf. Surv. Evol. Biol.* **2**, 28 (1985).
- T. Wenseleers, *J. Evol. Biol.* **19**, 1419, discussion 1426 (2006).
- A. Gardner, S. A. West, N. H. Barton, *Am. Nat.* **169**, 207 (2007).
- O. Leimar, P. Hammerstein, *J. Evol. Biol.* **19**, 1403, discussion 1426 (2006).
- S. A. West, S. P. Diggle, A. Buckling, A. Gardner, A. S. Griffin, *Annu. Rev. Ecol. Evol. Syst.* **38**, 53 (2007).
- P. E. Turner, L. Chao, *Nature* **398**, 441 (1999).
- J. E. Strassmann, Y. Zhu, D. C. Queller, *Nature* **408**, 965 (2000).
- G. J. Velicer, L. Kroos, R. E. Lenski, *Nature* **404**, 598 (2000).
- P. B. Rainey, K. Rainey, *Nature* **425**, 72 (2003).
- R. C. MacLean, I. Gudelj, *Nature* **441**, 498 (2006).
- S. P. Diggle, A. S. Griffin, G. S. Campbell, S. A. West, *Nature* **450**, 411 (2007).
- A. Ross-Gillespie, A. Gardner, S. A. West, A. S. Griffin, *Am. Nat.* **170**, 331 (2007).
- O. M. Gilbert, K. R. Foster, N. J. Mehdiabadi, J. E. Strassmann, D. C. Queller, *Proc. Natl. Acad. Sci. U.S.A.* **104**, 8913 (2007).
- R. Kümmerli, P. van den Berg, A. S. Griffin, S. A. West, A. Gardner, *J. Evol. Biol.* **23**, 699 (2010).
- Materials and methods are available as supporting material on Science Online.
- Moments of allele frequency distributions can also be expressed in terms of probabilities of identity by descent (IBD). For example, the second and third moments are proportional to the probabilities that two or three (respectively) randomly sampled alleles within a group are IBD (23).
- M. C. Whitlock, *Genetics* **160**, 1191 (2002).
- G. J. Velicer, M. Vos, *Annu. Rev. Microbiol.* **63**, 599 (2009).
- S. A. West, A. S. Griffin, A. Gardner, S. P. Diggle, *Nat. Rev. Microbiol.* **4**, 597 (2006).
- S. Wright, *Genetics* **16**, 97 (1931).
- P. Godfrey-Smith, B. Kerr, *Am. Nat.* **174**, 906 (2009).
- J. Smith, *Proc. Biol. Sci.* **268**, 61 (2001).
- S. P. Brown, S. A. West, S. P. Diggle, A. S. Griffin, *Philos. Trans. R. Soc. London B Biol. Sci.* **364**, 3157 (2009).
- R. H. Crozier, P. Pamilo, *Evolution of Social Insect Colonies* (Oxford Univ. Press, Oxford, 1996).
- We thank G. Velicer for funding and laboratory support through NIH grant GM07690 and S. Alizon, W. Castle, D. Queller, and W. Ratcliff for discussion and comments on the manuscript. J.D.V.D. was supported by NIH grant R01GM084238 to M.J. Wade. P.C.Z. was supported by the Genetics, Cellular and Molecular Sciences Training Grant (T32GM007757). All authors conceived the project, discussed the results, and commented on the paper. j.s. and D.V.D. designed the theoretical approach. j.s. did the math, designed and performed the experiments, and wrote the paper. j.s. and P.C.Z. analyzed the data.

#### Supporting Online Material

www.sciencemag.org/cgi/content/full/328/5986/1700/DC1  
Materials and Methods  
Figs. S1 to S4  
References

16 March 2010; accepted 18 May 2010  
10.1126/science.1189675

## c-di-AMP Secreted by Intracellular *Listeria monocytogenes* Activates a Host Type I Interferon Response

Joshua J. Woodward,<sup>1</sup> Anthony T. Iavarone,<sup>2</sup> Daniel A. Portnoy<sup>1,3\*</sup>

Intracellular bacterial pathogens, such as *Listeria monocytogenes*, are detected in the cytosol of host immune cells. Induction of this host response is often dependent on microbial secretion systems and, in *L. monocytogenes*, is dependent on multidrug efflux pumps (MDRs). Using *L. monocytogenes* mutants that overexpressed MDRs, we identified cyclic diadenosine monophosphate (c-di-AMP) as a secreted molecule able to trigger the cytosolic host response. Overexpression of the di-adenylate cyclase, *dacA* (*lmo2120*), resulted in elevated levels of the host response during infection. c-di-AMP thus represents a putative bacterial secondary signaling molecule that triggers a cytosolic pathway of innate immunity and is predicted to be present in a wide variety of bacteria and archaea.

The mammalian innate immune system is composed of receptors that collectively serve as a pathogen sensor to monitor the extracellular, vacuolar, and cytosolic cellular compartments (1). Recognition of microbes within these distinct compartments leads to cellular responses that are commensurate with the microbial threat. Although both pathogenic and non-pathogenic microbes interact with extracellular and vacuolar compartments, infectious disease

agents often mediate their pathogenesis by directly entering the cytosol or through delivery of virulence factors into the host cell cytosolic compartment. Thus, the innate immune system may distinguish between pathogenic and non-pathogenic microbes by monitoring the cytosol (2, 3).

Several distinct pathways of innate immunity are present in the host cell cytosol. One, termed the cytosolic surveillance pathway (CSP), detects bacterial, viral, and protozoan pathogens, leading to the activation of interferon regulatory factor 3 (IRF3) and nuclear factor kappa-light-chain-enhancer of activated B cells (NF- $\kappa$ B), resulting in the induction of interferon- $\beta$  (IFN- $\beta$ ) and co-regulated genes (4). Some ligands that activate this pathway are known, for example, viral and bacterial nucleic acids (5). However, the ligands

and host receptors that lead to IFN- $\beta$  production after exposure to nonviral microbes—including *L. monocytogenes*, *M. tuberculosis*, *F. tularensis*, *L. pneumophila*, *B. abortus*, and *T. cruzi*—remain unknown (4–9).

Expression of *L. monocytogenes* multidrug efflux pumps (MDRs) of the major facilitator superfamily controls the capacity of cytosolic bacteria to induce host expression of IFN- $\beta$  (10). Ectopic expression of multiple MDRs enhances IFN- $\beta$  production, while one, MdrM, controls the majority of the response to wild-type bacteria (10). Given that MDRs transport small molecules (<1000 daltons), we hypothesized that *L. monocytogenes* secretes a bioactive small molecule that is recognized within the host cell cytosol. To identify the bioactive ligand(s) secreted by *L. monocytogenes* MDRs, we performed solid phase extraction (SPE) of the culture supernatant from an MdrM overexpressing *L. monocytogenes* strain (*marR*-, DP-L5445) that exhibits an IFN- $\beta$  hyperactivating phenotype (11). Delivery of the fraction to the macrophage cytosol using reversible digitonin permeabilization (12) resulted in a dose-dependent increase in type-I IFN (Fig. 1A). Addition of this fraction in the absence of digitonin resulted in no IFN production, consistent with cytosolic detection of the active ligand.

In *L. monocytogenes* strains that exhibit variable levels of MDR expression, IFN- $\beta$  production correlates with increases in transporter levels (10). Supernatants from four *L. monocytogenes* strains—*mdrM*-, WT, *marR*-, and *tetR::Tn917*, each with increasing levels of MDR expression—were tested for activity. Comparable to infection assays, MDR expression correlated with IFN-inducing activity of the culture supernatants (Fig. 1B). The *tetR::Tn917* strain exhibited high-

<sup>1</sup>Department of Molecular and Cellular Biology, University of California, Berkeley, CA 94720, USA. <sup>2</sup>QB3/Chemistry Mass Spectrometry Facility, University of California, Berkeley, CA 94720, USA. <sup>3</sup>School of Public Health, University of California, Berkeley, CA 94720, USA.

\*To whom correspondence should be addressed. E-mail: portnoy@berkeley.edu



## Supporting Online Material for

### **A Generalization of Hamilton's Rule for the Evolution of Microbial Cooperation**

jeff smith,\* J. David Van Dyken, Peter C. Zee

\*To whom correspondence should be addressed. E-mail: [smith74@indiana.edu](mailto:smith74@indiana.edu)

Published 25 June 2010, *Science* **328**, 1700 (2009)

DOI: 10.1126/science.1189675

#### **This PDF file includes**

Materials and Methods  
Figs. S1 to S4  
References

## Supporting Online Material: Materials and Methods

**Derivation of the generalized Hamilton's rule.** Our analysis is a neighbor-modulated formulation of kin selection, which partitions fitness into the effect of an individual's own genotype and the effect of social neighbors ( $S1, S2$ ). We consider the situation in which there are two genotypes: a cooperator and a noncooperator. The social neighborhoods of these genotypes contain varying frequencies of cooperators. Social selection changes the abundance of the two strains, but mutation, recombination, and horizontal gene transfer are assumed rare enough to not significantly affect genotype frequencies.

Let the absolute fitness of a genotype be  $w = n'/n$ , where  $n$  and  $n'$  are the total number of individuals of that genotype before and after selection. Let the  $g$  be the genotypic value of individuals such that cooperators have  $g = 1$  and noncooperators  $g = 0$ . Let  $G$  be an individual's social environment—the frequency of cooperators among other members of the social group. Because we are interested in social evolution, the fitness of individuals is affected by both their own genotype and that of their neighbors:  $w = w(g, G)$ . Any smooth fitness function can be expanded in a Taylor series around  $(g = 0, G = 0)$  as

$$w = \sum_{j=0}^{\infty} b_j G^j + \sum_{k=0}^{\infty} d_k g G^k.$$

We let baseline fitness be  $b_0 = a$  and the cost of cooperation when all neighbors are noncooperators be  $d_0 = -c$ . The covariance between fitness and genotype  $\text{Cov}(w, g)$  ( $S1$ ) is then

$$\text{Cov}(a, g) + \sum_{j=1}^{\infty} b_j \text{Cov}(G^j, g) - c \text{Cov}(g, g) + \sum_{k=1}^{\infty} d_k \text{Cov}(g G^k, g).$$

Because  $a$  is a constant,  $\text{Cov}(a, g) = 0$ .  $\text{Cov}(g, g) = \text{Var}(g)$ . Dividing by  $\text{Var}(g)$ ,

$$\frac{\text{Cov}(w, g)}{\text{Var}(g)} = \beta_{wg} = \sum_{j=1}^{\infty} b_j \beta_{G^j g} - c + \sum_{k=1}^{\infty} d_k \beta_{(g G^k) g}.$$

We let  $r_j = \beta_{G^j g} = E(G_{\text{coop}}^j) - E(G_{\text{non}}^j) = m_j^{\text{coop}} - m_j^{\text{non}}$ , where  $m_j^{(i)}$  is the  $j$ th moment of the distribution of  $G$  around  $G = 0$  for genotype  $i$ . The regression definition of kin selection relatedness  $r = \beta_{Gg}$  ( $S1$ ) is equivalent to the first-order term  $r_1$ . Higher order terms  $r_j = \beta_{G^j g}$  can

be thought of as higher-order relatednesses. We can write the vector of moments as  $\mathbf{m}_i = \{m_1^{(i)}, m_2^{(i)}, \dots\}$  and the vector of relatednesses as  $\mathbf{r} = \{r_1, r_2, \dots\} = \mathbf{m}_{\text{coop}} - \mathbf{m}_{\text{non}}$ . If we let  $\mathbf{b} = \{b_1, b_2, \dots\}$  then  $\sum b_j \beta_{G^j_g} = \mathbf{r} \cdot \mathbf{b}$ . Similarly, we can write  $\beta_{(G^k)_g} = E(g_{\text{coop}} G^k_{\text{coop}}) - E(g_{\text{non}} G^k_{\text{non}}) = 1 \cdot E(G^k_{\text{coop}}) - 0 \cdot E(G^k_{\text{non}}) = m_k^{(\text{coop})}$ . If we let  $\mathbf{d} = \{d_1, d_2, \dots\}$  and  $\mathbf{m}_{\text{coop}} = \mathbf{m}$  then  $\sum d_k \beta_{(G^k)_g} = \mathbf{m} \cdot \mathbf{d}$ .

Selection favors cooperation when  $\beta_{wg} > 0$ . That is, when

$$\mathbf{r} \cdot \mathbf{b} - c + \mathbf{m} \cdot \mathbf{d} > 0. \quad (\text{S1})$$

In the special case where all fitness effects are completely additive (Fig. 1A),  $w = a + b_1 G - cg$ . Then  $\mathbf{b} = \{b_1, 0, 0, \dots\}$  and  $\mathbf{d} = \{0, 0, \dots\}$ . Substituting into equation (S1) recovers the standard expression for Hamilton's rule:  $r_1 b_1 - c > 0$ . Mean fitness is  $\bar{w} = \bar{g} E(w_{\text{coop}}) + (1 - \bar{g}) E(w_{\text{non}}) = \bar{g} [a - c + \mathbf{m} \cdot (\mathbf{b} + \mathbf{d})] + (1 - \bar{g}) [a + \mathbf{b} \cdot \mathbf{m}_{\text{non}}] = a + \mathbf{m}_{\text{non}} \cdot \mathbf{b} + \bar{g} \beta_{wg}$ .

**Bacterial strains.** *Myxococcus xanthus* strains were obtained from G. J. Velicer (Indiana University). GJV1 is a descendant of the standard laboratory strain DK1622 (S3). GJV10 (S4) is a derivative of GJV1 with an integrated pDW79 plasmid that confers resistance to kanamycin. In this paper we refer to GJV10 as the cooperator strain. GJV206.3 is a laboratory-evolved cheater strain that is resistant to rifampicin (S5). Strains were stored at  $-80^\circ\text{C}$  in 20% (v/v) glycerol.

**Sporulation assay.** Cells were grown in 8 ml CTT growth media (S3) at  $32^\circ\text{C}$  while shaking at 300 rpm. Log-phase cells were centrifuged 15 min at  $4500 \times g$  and resuspended in TPM starvation media to a density of  $5 \times 10^9$  cells/ml. Resuspended cells were mixed at cooperator frequencies of 0%, 1%, 10%, 50%, 90%, 99%, or 100% of total cells.  $100 \mu\text{l}$  ( $5 \times 10^8$  cells/ml) of each cell suspension was plated onto 1.5% TPM agar. Cells developed for 5 days at  $32^\circ\text{C}$  and 90% rh. Fruiting bodies were harvested with a sterile scalpel into 1 ml dH<sub>2</sub>O, heated 2 hr at  $50^\circ\text{C}$  to kill any remaining vegetative cells, and then sonicated to disperse spores. Spores were serially diluted in dH<sub>2</sub>O and plated in 0.5% CTT agar. Densities of GJV10 spores were measured from colony counts on plates containing  $40 \mu\text{g/ml}$  kanamycin (Sigma, St. Louis). Densities of GVB206.3 spores were measured from colony counts on plates containing  $5 \mu\text{g/ml}$  rifampicin (Sigma, St. Louis). Replicate experimental blocks were conducted on separate days with cells grown independently from the same frozen stock. For each strain, absolute fitness during development is equivalent to sporulation efficiency: the number of cells surviving as

spores divided by the number of cells plated. The inclusive fitness effect was calculated as mean cooperator fitness minus mean cheater fitness.

**Statistics and calculations.** All statistics and calculations were performed using R 2.8.1 (R Development Core Team, Vienna, Austria, <http://www.R-project.org>) unless otherwise indicated. The equation for developmental fitness was determined by ANCOVA (1m procedure) on  $\log_{10}$ -transformed fitness data. The best-fit statistical model included significant terms for intercept, slope ( $G$ ), genotype effect on intercept ( $g$ ), slope by genotype interaction ( $g \times G$ ), and a quadratic term ( $G^2$ ).  $w(g, G)$  was obtained by transforming the fitted regression equation to a linear fitness scale.

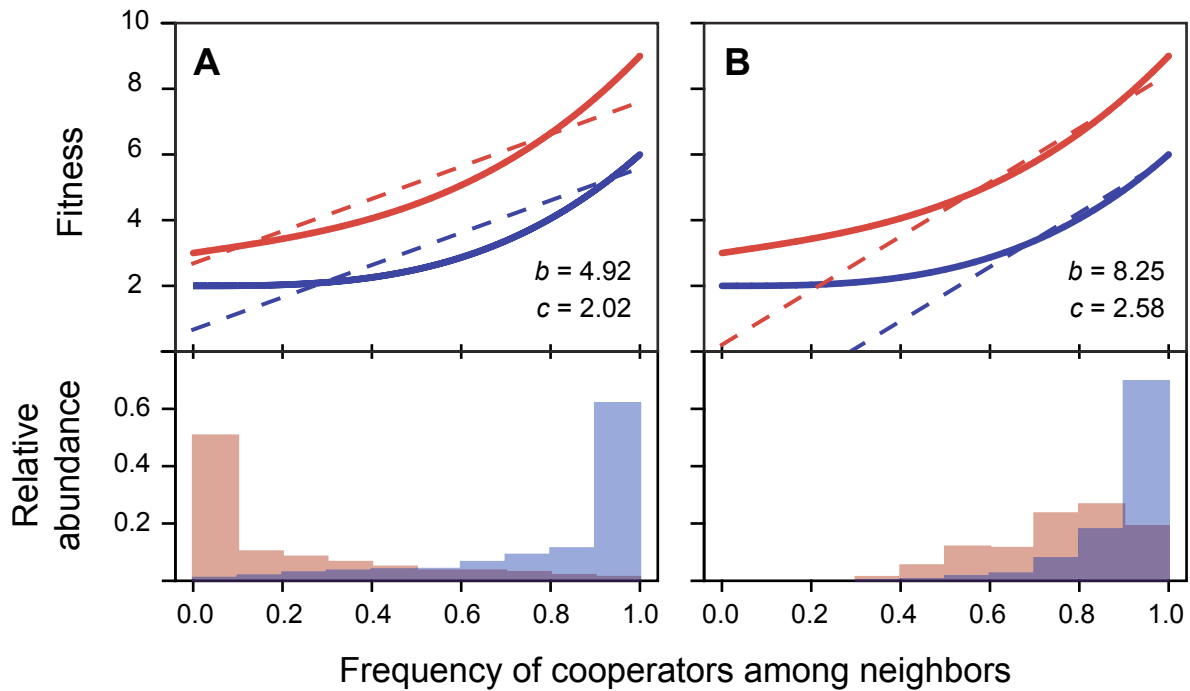
Values of  $a$ ,  $\mathbf{b}$ ,  $c$ , and  $\mathbf{d}$  were determined from the coefficients of the Taylor series of  $w(g, G)$  up to order 30, obtained using the `Series` command in Mathematica 7.0 (Wolfram Research, Champaign, IL). We emphasize that we did not fit a 30-order polynomial to our data; we simply represented its five-parameter statistical model in terms of its Taylor series. The different components of  $\mathbf{b}$  and  $\mathbf{d}$  are not independent of each other.  $\mathbf{m}$ ,  $\mathbf{m}_{\text{non}}$ , and  $\mathbf{r}$  were calculated from the moments of the experimental distribution. If  $G$  is the initial frequency of cooperators among developing cells within a group, then moment  $k$  of genotype  $i$  was calculated as  $E(G^k)$ , where the expectation is taken over all cells of genotype  $i$ . The inclusive fitness effect  $\beta_{wg}$  was calculated as in equation (S1). Error estimates were determined by bootstrap. Coefficients of the full statistical model were determined for 1000 instances of resampled data. For each of these equations,  $a$ ,  $\mathbf{b}$ ,  $c$ ,  $\mathbf{d}$ , and  $\beta_{wg}$  were calculated as described above.

Lacking empirical data on the distribution of genotypes among naturally occurring *M. xanthus* fruiting bodies, we assumed for convention's sake an island model of population structure (S6) in which genotypes follow a beta distribution among groups (Fig. S2, for example). Beta distributions of within-group cooperator frequency were implemented using the `dbeta` command in R with parameters  $\alpha = 2Nm\bar{g}$  and  $\beta = 2Nm(1-\bar{g})$ , where  $\bar{g}$  is the global cooperator frequency and  $2Nm$  is a distribution parameter. These were then normalized to obtain the distribution of  $G$  for each genotype separately:  $G \text{ dbeta}(G)/\bar{g}$  for cooperators and  $(1-G) \text{ dbeta}(G)/(1-\bar{g})$  for noncooperators. Moments  $m_k^{(i)}$  were calculated by numerically integrating  $G^k$  over the probability distribution of genotype  $i$ . We varied the migration parameter  $2Nm$  but

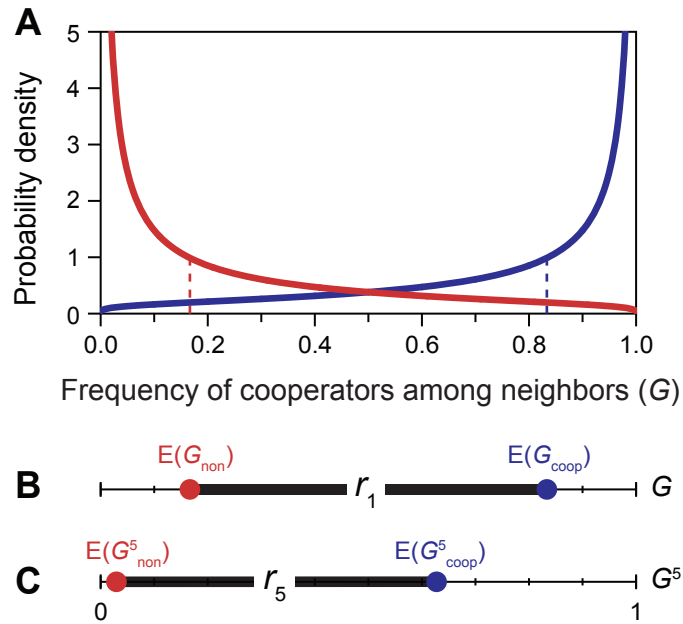


report population structure in terms of first-order relatedness for ease of comparison. For each combination of parameters we calculated the inclusive fitness effect and mean fitness as described above.

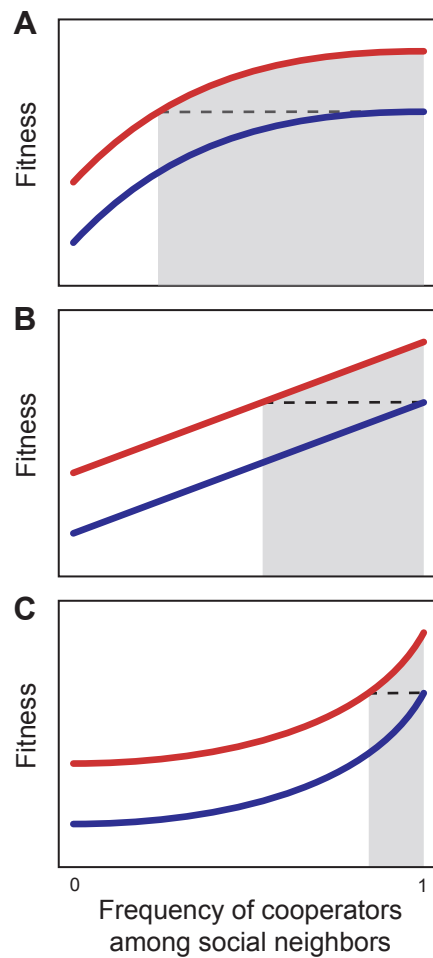
To determine the fit of Hamilton's rule to nonadditive data, we simulated island models of population structure with 500 groups of 100 individuals using the `rbeta` command in R and other parameters as described above. Each individual was assigned a fitness based on its own genotype and that of its neighbors using the fitness functions described in the text. Hamilton's rule was then fit to these distributions as a partial regression with fitness structure  $w = a - cg + bG$  using the `lm` command.



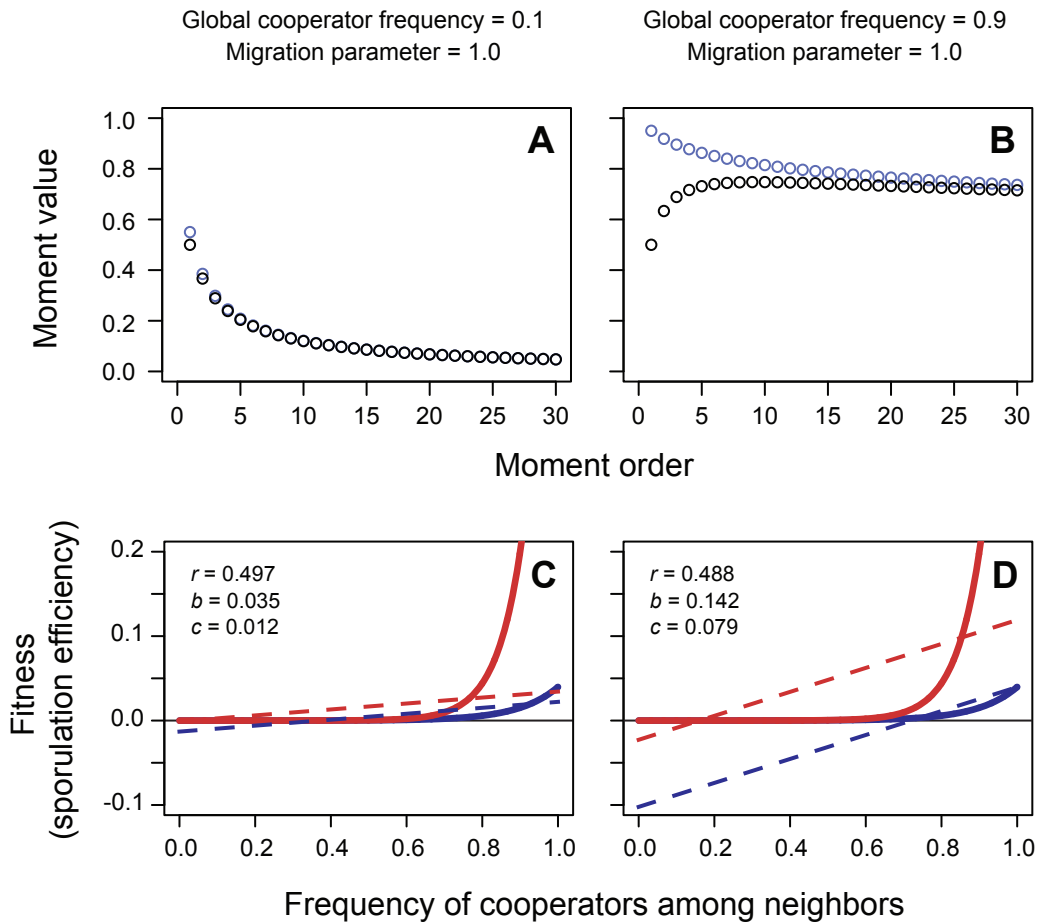
**Supplementary Figure 1.** Limitations of Hamilton's rule with strong nonadditivity. Solid lines in the top panels show an example nonadditive fitness function. Dashed lines show the fitness function estimated by Hamilton's rule given the distribution shown in the bottom panel. Blue: cooperators. Red: noncooperators. Hamilton's rule is effectively a linear regression fit to nonlinear data. This limits the amount of variation it can explain and in some cases leads to biologically nonsensical results like negative mean fitness at some cooperator frequencies [dashed blue line in (B)]. Hamilton's rule also confounds fitness effects with population structure: it identifies different  $b$  and  $c$  values for (A) and (B) even though they have identical fitness functions.



**Supplementary Figure 2.** Kin selection relatedness in asexual microbes. (A) Hypothetical distributions of cooperative genotypes among the social neighbors of cooperators (solid blue line) and noncooperators (solid red line). Dashed lines show distribution means. (B) The  $r$  in Hamilton's rule is  $r_1$ : the difference between the means of the distributions. (C) Higher order relatednesses are the differences between the higher-order moments of the distributions. Shown is fifth-order relatedness  $r_5$ .



**Supplementary Figure 3.** The functional form of nonadditive benefits determines the range of social groups in which cheaters gain a net fitness advantage over cooperators. Red line: cheater fitness. Blue line: cooperator fitness. Shaded area: cheaters have greater fitness than cooperators in all-cooperator social groups. (A) Decreasing returns from cooperation. (B) Linear returns. (C) Increasing returns. Larger shaded areas require more population structure to prevent invasion of cheaters.



**Supplementary Figure 4.** Identifying the causes of frequency-dependent social selection. (A, B) In the island model of population structure, kin selection relatedness ( $r_1$ ) is independent of global cooperator frequency, but  $r$  (black) and  $m$  (blue) are not. Because selection in the *Myxococcus* example is dominated by terms of order 10-15, it is these components of population structure that create frequency-dependent selection. (C, D) Hamilton's rule misleadingly places the cause of frequency-dependent selection in its fitness terms ( $b$  and  $c$ ) instead of its population structure term ( $r$ ). Solid lines show the *Myxococcus* fitness function estimated in Fig. 2A, now plotted on a linear scale. Dashed lines show the fitness function estimated by Hamilton's rule for the population structures in the panels above. The small difference in  $r$  between (C) and (D) is caused by randomness in the simulated population structures.

## Supplementary References

- S1. D. C. Queller, *Evolution* **46**, 376-380 (1992).
- S2. P. D. Taylor, S. A. Frank, *J. Theor. Biol.* **180**, 27-37 (1996).
- S3. D. Kaiser, *Proc. Natl. Acad. Sci. U.S.A.* **76**, 5952-5956 (1979).
- S4. F. Fiegna, G. J. Velicer, *Proc. R. Soc. London Ser B* **270**, 1527-1534 (2003).
- S5. G. J. Velicer, L. Kroos, R. E. Lenski, *Nature* **404**, 598-601 (2000).
- S6. S. Wright, *Genetics* **16**, 97-159 (1931).